

Porous Cationic Electrospun Fibers with Sufficient Adsorption Sites for Effective and Continuous $^{99}\text{TcO}_4^-$ Uptake

Rui Zhao, Dingyang Chen, Nvwa Gao, Liyong Yuan, Wei Hu, Fengchao Cui, Yuyang Tian,* Weiqun Shi,* Shengqian Ma, and Guangshan Zhu*

Removal of radioactive technetium-99 ($^{99}\text{TcO}_4^-$) from water by effective adsorbents is highly desired but remains a challenge. The currently used resin adsorbents possess several obstacles, such as slow adsorption kinetics and low adsorption capacity. To address these issues, herein a type of fibrous adsorbent with porosity and hyper-branched quaternary ammonium groups, namely porous cationic electrospun fibers (PCE fibers), is successfully prepared. PCE fibers can remove 97% of $^{99}\text{TcO}_4^-$ within 1 min and the equilibrium time of 99% removal is 20 min. The predicted maximum adsorption capacity toward the surrogate ReO_4^- can reach 826 mg g^{-1} , which is higher than the state of art anion-exchange resins and most of the other reported adsorbents. Furthermore, PCE fibers have good selectivity for ReO_4^- in the presence of competitive anions, and can retain ReO_4^- uptake under extreme conditions including high acid–base and gamma irradiation. Importantly, PCE fibrous adsorptive membrane is employed for dynamic ReO_4^- removal from simulated Hanford LAW stream with a processing capacity of 600 kg simulated stream per kilogram PCE fibers. The excellent performance highlights the advantages of PCE fibers over traditional resins in technetium removal.

produced from the nuclear fission of uranium-235 and plutonium-239 with a high fission yield of $\approx 6.1\%$.^[5] Due to its long half-life (2.1×10^5 years), high water solubility (existed in the form of pertechnetate anions, $^{99}\text{TcO}_4^-$), and almost noncomplexing nature, ^{99}Tc has a fast migration in the environment and easily enters into local ecological systems, resulting in a serious environmental concern. Moreover, ^{99}Tc also disturbs the extraction of uranium, neptunium, and plutonium through its catalytic redox activity, and the volatile tendency of $^{99}\text{TcO}_4^-$ to $^{99}\text{Tc}_2\text{O}_7$ during nuclear waste vitrification process leads to a risk of leakage.^[6–9] Therefore, the capture of $^{99}\text{TcO}_4^-$ is critical and significant for nuclear fuel retreatment and environmental remediation.

To address this challenging issue, cationic solid adsorbents with easy operation, low cost, good selectivity, and high stability properties are considered as promising

1. Introduction


Nuclear power with high energy output is a competitive power supply in the context of global energy shortage.^[1,2] However, the associated radioactive pollution in certain types of nuclear waste streams brings severe threats toward the environmental system and human health.^[3,4] Among the radioisotope contaminations, technetium-99 (^{99}Tc) is a β -emitting radionuclide

materials for separating anionic $^{99}\text{TcO}_4^-$ via the ion exchange process.^[10] Considering the danger of handling radioactive $^{99}\text{TcO}_4^-$ in general laboratories, ReO_4^- is usually used as a nonradioactive analog for $^{99}\text{TcO}_4^-$.^[11] Traditional microspherulitic polymeric anion-exchange resins (e.g., IRA-400, IRA-401 or Purolite-A-520E) have already been applied for $^{99}\text{TcO}_4^-$ elimination in a practical large-scale treatment process. However, they showed slow adsorption kinetics and limited adsorption capacity due to their high mass transfer resistance and low content of functional groups.^[12] Thus, a series of new adsorbents have been explored to replace traditional resin beads. For example, inorganic cationic materials with easy preparation and low costs such as layered double hydroxide (LDH), $\text{Yb}_3\text{O}(\text{OH})_6\text{Cl}$, and thorium borates (NDTB-1) exhibited $^{99}\text{TcO}_4^-/\text{ReO}_4^-$ adsorption ability, but their relatively low uptake capacity and poor selectivity limited the practical applications.^[13–15] Recently, advanced porous materials such as metal–organic frameworks (MOFs), covalent organic frameworks (COFs), and cationic polymer networks (CPNs) with cationic adsorptive sites have been designed and investigated for $^{99}\text{TcO}_4^-/\text{ReO}_4^-$ removal, which showed high uptake capacity, fast kinetics, and excellent selectivity.^[16–18] However, the powder form of these materials makes them difficult to be used in practical dynamic separation and also difficult for recycling. Additionally, they also have high preparation cost. Therefore, the development of superior $^{99}\text{TcO}_4^-/\text{ReO}_4^-$ adsorbents integrating the properties of the aforementioned materials with good engineering form,

R. Zhao, D. Chen, N. Gao, W. Hu, F. Cui, Y. Tian, G. Zhu
Faculty of Chemistry
Northeast Normal University
Changchun 130024, P. R. China
E-mail: tianyy100@nenu.edu.cn; zhugs100@nenu.edu.cn

L. Yuan, W. Shi
Laboratory of Nuclear Energy Chemistry
Institute of High Energy Physics
Chinese Academy of Sciences
Beijing 100049, P. R. China
E-mail: shiwq@ihep.ac.cn

S. Ma
Department of Chemistry
University of North Texas
Denton, TX 76201, USA

 The ORCID identification number(s) for the author(s) of this article can be found under <https://doi.org/10.1002/adfm.202200618>.

DOI: 10.1002/adfm.202200618

low-cost, fast adsorption kinetics, high capacity, excellent selectivity, and satisfactory stability is urgently desired.

In contrast to the resin beads, polymeric fibers with easily handling availability, low mass transfer resistance, and high accessible surface would be much more suitable for $^{99}\text{TcO}_4^-/\text{ReO}_4^-$ capture from nuclear waste. They are also a type of adsorbent materials with macroscopic morphology and large-scale application potential. Nonetheless, the employment of polymeric fibers for $^{99}\text{TcO}_4^-/\text{ReO}_4^-$ removal remains unexplored to date. Electrospinning technology is an efficient method to fabricate various polymeric fibers with micro/nanoscale diameters. The obtained electrospun fibers feature some advantages such as easy preparation, high porosity, facile functionalization, low cost, and easy regeneration.^[19–21] Together with these attractive properties, electrospun fibers are competitive fibrous adsorbents or adsorptive membranes for contaminant removal from water.^[22–24] To improve the selectivity of pure electrospun polymer fibers, grafting specific binding sites is a straightforward strategy.^[25,26] For instance, amidoxime groups have been grafted onto electrospun polyacrylonitrile fibers for uranium extraction.^[27–29] However, one cyano group is usually converted into only one functional group and the maximum graft efficiency is limited. In addition, the grafting groups are modified only onto the surfaces of electrospun fibers but their interior is inaccessible, which further leads to a limited grafting density. Therefore, increasing the accessibility and the density of cationic sites in electrospun fibers should be a promising approach to enhance the binding ability between fibrous adsorbents and $^{99}\text{TcO}_4^-/\text{ReO}_4^-$ thereby high uptake capacity, fast removal rate, and good selectivity. Nonetheless, current electrospun fiber adsorbents cannot meet the above requirements. Studies focused on the rational design of electrospun fibers with desired physical and chemical structures possessing good $^{99}\text{TcO}_4^-/\text{ReO}_4^-$ adsorption performances are meaningful for chemical science and materials engineering.

In this study, to improve the grafting density and the utilization of the cationic functional groups in electrospun fibers, pore-forming inside the fibers and hyperbranched graft modification were combined to fabricate porous cationic electrospun fibers (PCE fibers) for $^{99}\text{TcO}_4^-/\text{ReO}_4^-$ removal from water. Constructing porous structures in the fibers exposed more accessible basal groups (cyano groups) for functional group grafting, and these pores also decreased the mass transfer resistance and accelerate the adsorption kinetics. Hyperbranched graft modification converted one cyano group into multiple functional groups, resulting in the increased grafting density. Cationic N-contained groups were usually applied as the functional groups for $^{99}\text{TcO}_4^-/\text{ReO}_4^-$ adsorption.^[16,30–32] Considering the operational availability of the grafting reaction, quaternary ammonium group was chosen as the functional group in this work. As expected, the obtained PCE fibers could efficiently capture $^{99}\text{TcO}_4^-/\text{ReO}_4^-$ with fast kinetics, high capacity, excellent selectivity, and good stability. The interaction between PCE fibers and ReO_4^- was also well investigated, suggesting that the superior adsorption performance of PCE fibers is due to the hyperbranched cationic quaternary ammonium groups and pore structures in the fibers. This work thereby puts forth a promising material for $^{99}\text{TcO}_4^-/\text{ReO}_4^-$ removal from water.

2. Results and Discussion

2.1. Fibrous Adsorbent Design, Preparation, and Characterization

The porous cationic electrospun fibers (PCE fibers) for $^{99}\text{TcO}_4^-$ adsorption were prepared through three steps (Figure 1). Polyacrylonitrile (PAN) was selected as the polymer substrate because it contains numerous cyano groups that can be transformed into various functional moieties. Porous electrospun polyacrylonitrile fibers (PPAN fibers) were first fabricated through the removal of pore template polyvinylpyrrolidone (PVP) from electrospun PAN/PVP/CNTs blending fibers. Carbon nanotubes (CNTs) were added into the fibers to improve the mechanical property that is confirmed by the stress–strain curves (Figure S1, Supporting Information). Then, branched polyethylenimine (PEI) with a large number of amine groups ($-\text{NH}_2$, $-\text{NH}-$, $-\text{N}<$) as quaternary ammonium precursors were grafted onto PPAN fibers via the hydrothermal reaction and gave the PEI-PPAN fibers. Finally, porous cationic electrospun fibers (PCE fibers) with anion exchange capacity were successfully prepared after the quaternization reaction of PEI-PPAN fibers with bromoethane and the following ion exchange process to replace toxic Br^- with Cl^- .

The macroscopic optical photo of PCE fibers is shown in Figure S2 (Supporting Information) and the microstructure of PCE fibers were observed by SEM. The PCE fibers were long and continuous with an average diameter of 207 nm (Figure 2a; Figure S3, Supporting Information). After the pore template removal and the grafting reactions, porous structures were formed on the fibers and the surfaces of the fibers became coarser (Figure S4, Supporting Information). Distinct pores were observed in the fibers (Figure 2b) and the BET surface area of PCE fibers was $64.2 \text{ m}^2 \text{ g}^{-1}$ caused by the extra inner surfaces created by pore formation (Figure 2c). Inset in Figure 2c showed obvious mesopore distribution of PCE fibers. The chemical structures and compositions of the obtained fibers were studied. As shown in the FT-IR results (Figure 2d), the peak at 2240 cm^{-1} belonging to $-\text{C}\equiv\text{N}$ bond almost disappears in the spectrum of PEI-PPAN fibers and a new peak at 1652 cm^{-1} reveals the $\text{C}=\text{O}$ stretching of amide groups. Moreover, the broad peak at $\approx 3400 \text{ cm}^{-1}$ is assigned to $\text{N}-\text{H}$ stretching bond. These results provide the evidence of the grafting of branched polyethylenimine onto PPAN fibers.^[33] After the quaternization reaction, the peaks at 2946 and 2834 cm^{-1} that are the typical $\text{C}-\text{H}$ stretching vibrations of $-\text{CH}_2-$ or $-\text{CH}_3$ groups become stronger because of the reaction with bromoethane.^[34,35] The intensity for $\text{N}-\text{H}$ stretching at 3400 cm^{-1} is retained, suggesting that most of the bromoethane reacts with tertiary amines on PEI. The structure of PCE fibers was also estimated by solid-state ^{13}C cross-polarization magic angle spinning (CP/MAS) NMR. The carbon signals are consistent with the compositions of PCE fibers (Figure S5, Supporting Information). The peaks at 55.7 and 65.9 ppm correspond to carbon atoms next to the quaternary ammonium.^[36] The peak at 14.5 ppm is ascribed to methyl carbon. Moreover, the signals belonging to carbon atoms next to tertiary amine, secondary amine, primary amine, and amino are also observed in the spectrum. The quaternization reaction was

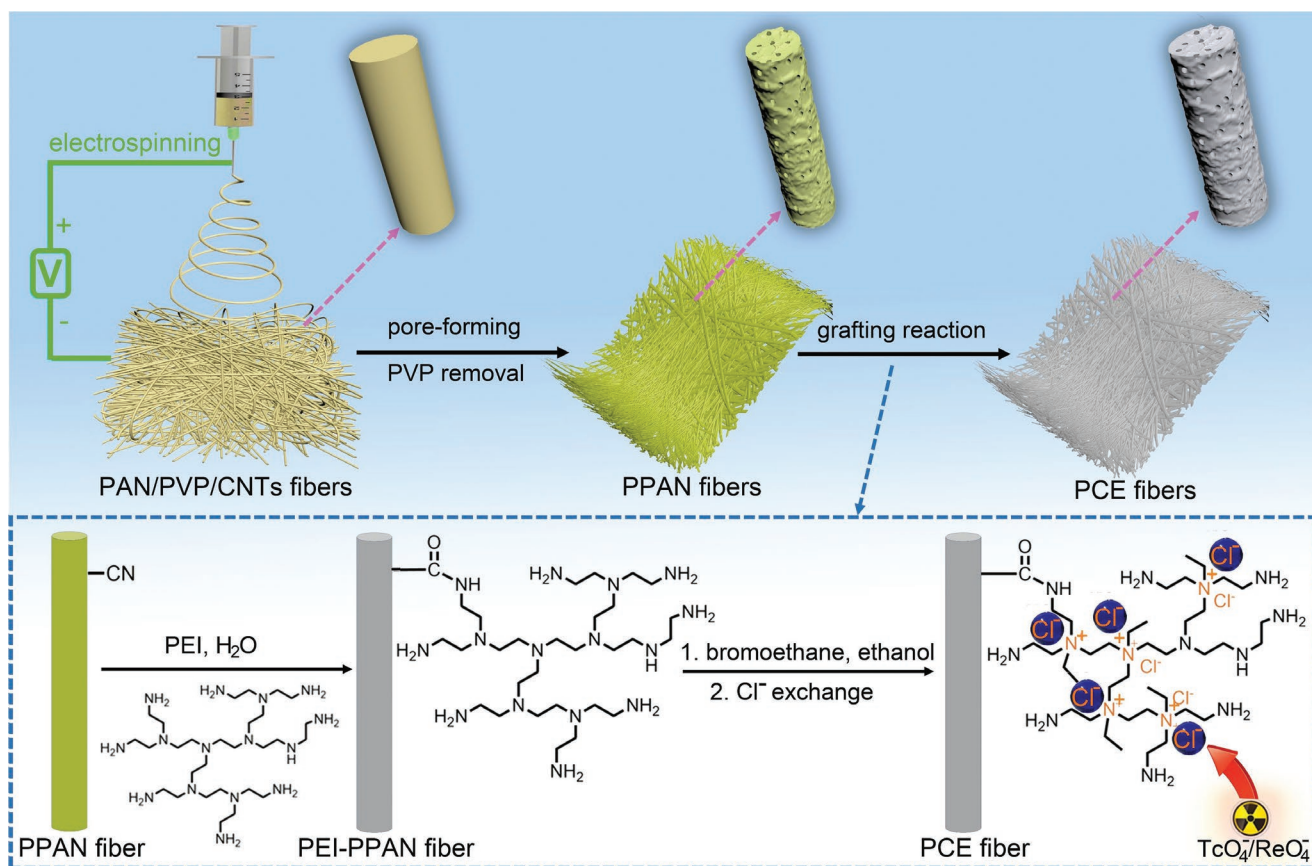


Figure 1. Schematic illustration of preparation route for porous cationic electrospun fibers (PCE fibers).

further confirmed by X-ray photoelectron spectroscopy (XPS; Figure 2e). Compared with the N 1s high-resolution scan of PEI-PPAN fibers showing only one peak at 398.5 eV (Figure S6, Supporting Information), the N 1s spectra of PCE fibers can be deconvoluted into at 398.8 and 400.8 eV that belong to non-quaternary nitrogen and quaternary nitrogen (Figure 2f),^[37] respectively, suggesting that quaternary ammonium groups are synthesized via the reaction of bromoethane and tertiary amine from PEI. In addition, the XPS survey spectrum of PCE fibers show Cl 2p peak without Br 3d peak indicating the nearly total exchange of Br⁻ by Cl⁻. The elemental composition of PCE fibers was further verified by energy-dispersive X-ray spectroscopy (EDS), elemental mapping, and elemental analysis results (Figures S7 and S8 and Table S1, Supporting Information). The ion exchange capacity (IEC) was also measured (the method is displayed in the Supporting Information) and PCE fibers with an IEC value of 3.47 mmol g⁻¹ was determined. The IEC value is higher than those of common anion exchange materials^[38–40] because the branched structure of PEI and constructed porous structures can provide abundant quaternization sites. For comparison, the IEC of cationic electrospun fibers (CE fibers) without porous structures (for details about their preparation, see the Supporting Information) was also measured, which is only 1.63 mmol g⁻¹. The high IEC value endows the PCE fibers with potential effective ⁹⁹TcO₄⁻/ReO₄⁻ cleanup performance. Actually, we have systematically investigated the preparation of PCE fibers through changing the PVP/PAN weight ratio,

hydrothermal reaction time, and quaternization reaction time (Figures S9 and S10, Supporting Information) in the preliminary experiments. The PCE fibers used in the characterization and performance test were the optimal results.

2.2. ⁹⁹TcO₄⁻/ReO₄⁻ Adsorption Performance

Encouraged by the above results, the adsorption performance of PCE fibers toward ⁹⁹TcO₄⁻ was investigated by adding 10 mg fiber adsorbents into a 20 ml aqueous solution containing 12.5 ppm real ⁹⁹TcO₄⁻. The concentration of ⁹⁹TcO₄⁻ was detected by the liquid scintillation counting measurements (Table S2, Supporting Information). PCE fibers showed surprisingly fast adsorption kinetics: at 1 min, 97% of ⁹⁹TcO₄⁻ were removed and the adsorption equilibrium reached within 20 min with >99% removal (Figure 3a). The removal kinetics of PCE fibers is significantly faster than that of two classical anion-exchange resins for ⁹⁹TcO₄⁻ removal (A532E and A530E).^[7] Considering the high radioactivity and limited availability of ⁹⁹TcO₄⁻, ReO₄⁻ having identical charge density with ⁹⁹TcO₄⁻ was applied as a nonradioactive surrogate in the following adsorption experiments, which have been proved to be feasible.^[4–6] The adsorption kinetics of PCE fibers toward ReO₄⁻ had similar tendency as ⁹⁹TcO₄⁻ (Figure 3a). Additionally, the adsorption of ReO₄⁻ by PCE fibers was carried out at a high concentration (25 ppm) and two commercial anion exchange resins (A520E and IRA-401)

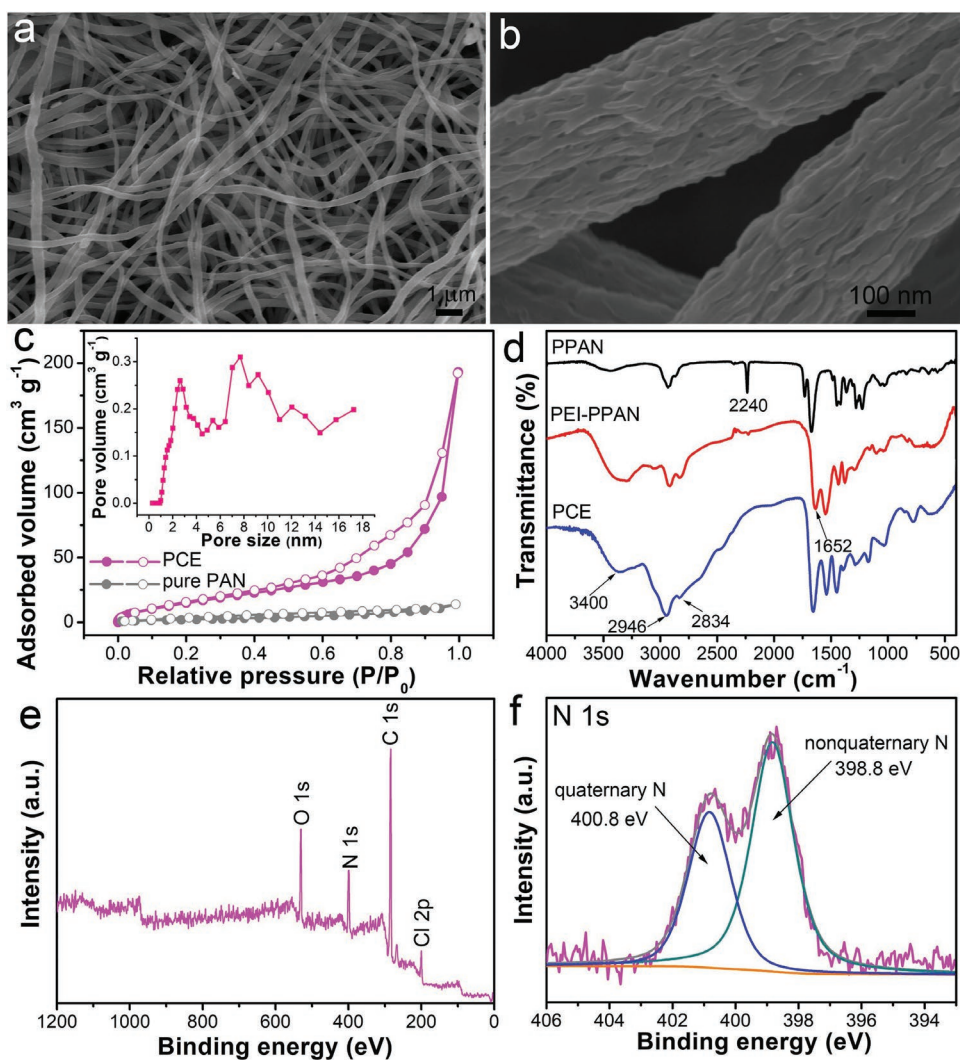


Figure 2. a,b) SEM images of PCE fibers. c) N_2 adsorption–desorption isotherms of PCE fibers and pure PAN fibers (inset is the pore-size-distribution of PCE fibers). d) FT–IR spectra of PPAN, PEI-PPAN, PCE fibers. e) XPS survey spectrum of PCE fibers. f) N 1s core-level spectra of PCE fibers.

were also tested to adsorb ReO_4^- for comparison. The equilibrium time for PCE fibers under these adsorption conditions was also 20 min. However, only 23.0% and 32.2% of ReO_4^- were removed by A520E and IRA-401 in 20 min, respectively, and it took 300 min (for A520E) and 360 min (for IRA-401) to reach the uptake equilibrium (Figure 3b). We further conducted the adsorption of PCE fibers toward ReO_4^- at a higher concentration of 50 ppm to quantify the kinetics (Figure S11, Supporting Information). Under these conditions, the adsorption equilibrium time was still 20 min and the adsorption process followed the pseudo-second order model better. Note that the fast adsorption kinetics of PCE fibers surpass almost all of reported shapeable adsorbents and are comparable to some of advanced porous materials (Figure 3g; Table S4, Supporting Information). The high content of quaternary ammonium groups provided abundant sites for $^{99}TcO_4^-/ReO_4^-$ binding and the porous microstructures of the fibers effectively decreased the mass transfer resistance. They both contributed to the rapid $^{99}TcO_4^-/ReO_4^-$ elimination. After the adsorption kinetics

(Figure 3b), the residual concentration of ReO_4^- in the solution was 0.089 mg L^{-1} (89 ppb). Thus, the calculated distribution coefficient (K_d) of PCE fibers for ReO_4^- adsorption reached $3.1 \times 10^5 \text{ mL g}^{-1}$, having the same order of magnitude as most of advanced cationic framework materials, including SCU-COF-1 ($3.9 \times 10^5 \text{ mL g}^{-1}$),^[16] ImPOP-1 ($3.2 \times 10^5 \text{ mL g}^{-1}$),^[32] SCP-IHEP-1 ($2.6 \times 10^5 \text{ mL g}^{-1}$),^[8] SCU-100 ($1.9 \times 10^5 \text{ mL g}^{-1}$),^[14] and VBCOP ($4.0 \times 10^5 \text{ mL g}^{-1}$),^[41] which indicates the strong affinity between PCE fibers and ReO_4^- . To demonstrate the effect of abundant functional groups and porous structures, a comparative adsorption experiment was conducted. Compared with CE fibers without porous structures, PCE fibers showed faster adsorption rate and higher uptake capacity due to the effect of porous structures that result in high grafting density and abundant transfer channels (Figure S12a, Supporting Information). In comparison, PEI-PPAN fibers without cationic sites had lower adsorption performance (Figure S12b, Supporting Information), indicating that quaternary ammonium groups play a major role in the adsorption of ReO_4^- via ion-exchange process.

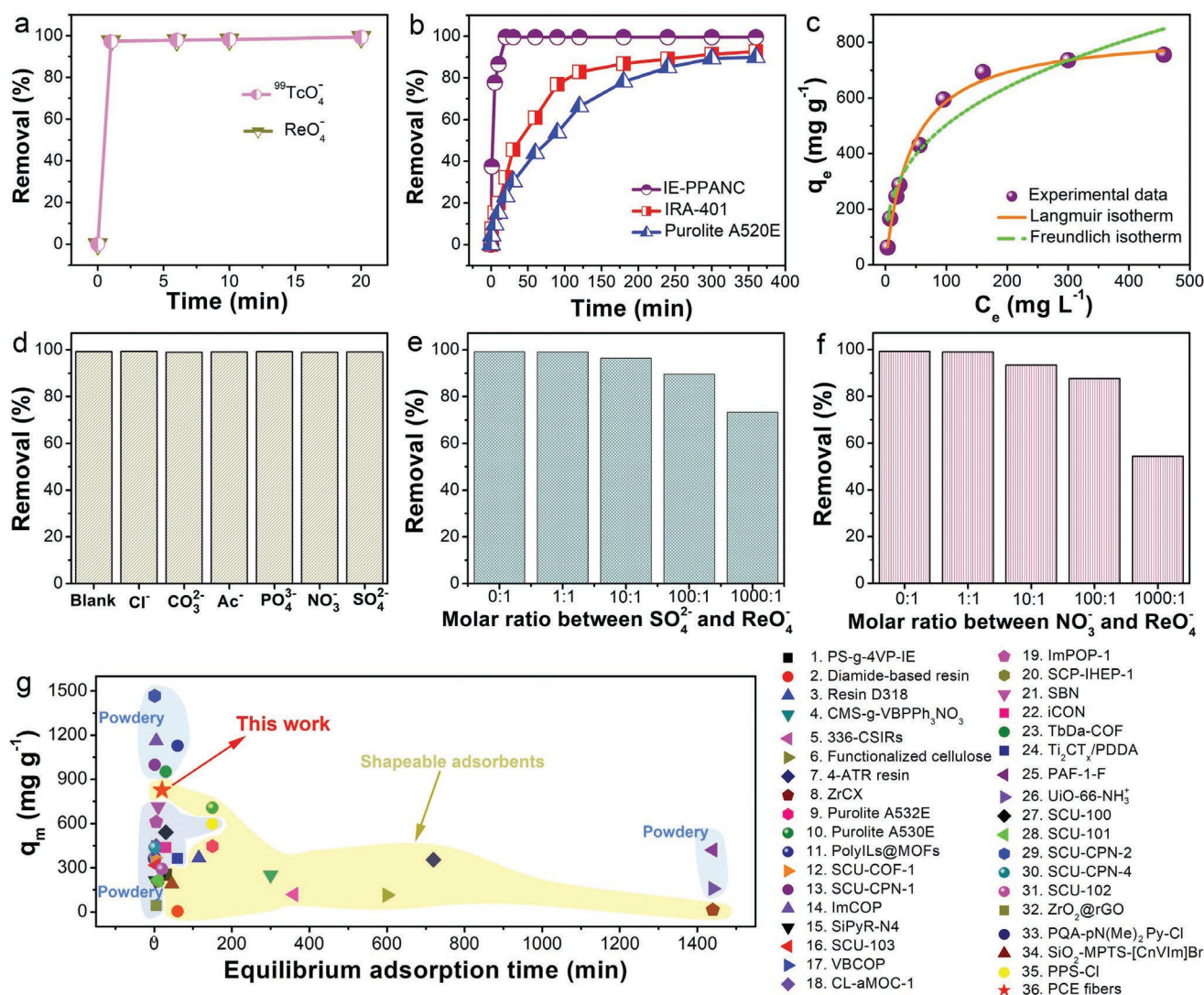


Figure 3. a) Adsorption kinetics of $^{99}\text{TcO}_4^-$ and ReO_4^- by PCE fibers ($C_0 = 12.5 \text{ mg g}^{-1}$, $m_{\text{adsorbent}}/V_{\text{solution}} = 0.5 \text{ g L}^{-1}$, pH 7.0). b) Adsorption kinetics of ReO_4^- by PCE fibers, IRA-401, and A520E ($C_0 = 25.0 \text{ mg g}^{-1}$, $m_{\text{adsorbent}}/V_{\text{solution}} = 0.5 \text{ g L}^{-1}$, pH = 7.0). c) Adsorption isotherm of PCE fibers toward ReO_4^- ($m_{\text{adsorbent}}/V_{\text{solution}} = 0.5 \text{ g L}^{-1}$, pH 7.0, $t = 12 \text{ h}$). d) Effect of different competing anions on ReO_4^- removal by PCE fibers ($C_0 = 25.0 \text{ mg g}^{-1}$, $m_{\text{adsorbent}}/V_{\text{solution}} = 1.0 \text{ g L}^{-1}$, pH = 7.0, $t = 6 \text{ h}$). Effect of excess e) SO_4^{2-} and f) NO_3^- on the removal of ReO_4^- ($C_0 = 25.0 \text{ mg g}^{-1}$, $m_{\text{adsorbent}}/V_{\text{solution}} = 1.0 \text{ g L}^{-1}$, pH 7.0, $t = 12 \text{ h}$). g) Comparison of ReO_4^- equilibrium adsorption time and maximum adsorption capacity of various reported adsorbents and their corresponding references are given in Table S3 (Supporting Information).

The adsorption capacity and the interaction of PCE fibers toward ReO_4^- were studied by adsorption isotherm. Langmuir model gave a better fitting correlation of the isotherm data ($R^2 = 0.9979$; Figure 3c; Figure S13 and Table S5, Supporting Information), suggesting that the adsorption sites on PCE fibers are homogeneous.^[22] The predicted maximum adsorption capacity based on Langmuir model was 826 mg g^{-1} and the high capacity was due to the abundant quaternary ammonium groups. According to the above results, the theoretical adsorption capacity of PCE fibers should be 868 mg g^{-1} (3.47×250) if all the quaternary ammonium groups were occupied by ReO_4^- . The results indicated that 95.2% of the quaternary ammonium groups were involved in the adsorption. The posttreatment grafting reaction for PCE fibers makes the functional groups on the surfaces or in the porous structures of the fibers,

which leads to the high utilization of the quaternary ammonium groups. The sufficient ion-exchange process from Cl^- to ReO_4^- was further confirmed by SEM-EDS spectrum and the elemental mapping (Figures S14 and S15, Supporting Information). The adsorption capacity of 826 mg g^{-1} PCE fibers is superior to those of commercial anion-exchange resins and shapeable adsorbents, and most of reported powdery cationic porous materials (Figure 3g; Table S6, Supporting Information). Recently, cationic organic network materials showed high ReO_4^- uptake capability exceeding PCE fibers, such as TbDa-COF (952 mg g^{-1}),^[6] SCU-CPN-1 (999 mg g^{-1}),^[7] ImCOP (1162 mg g^{-1}),^[31] and SCU-CPN-2 (1467 mg g^{-1}).^[18] However, compared with powdery cationic organic networks, PCE fibers with membranous engineering form is more suitable for practical application, which is favorable to recycling and can be

used in dynamic adsorption. The recycling capacity of PCE fibers was evaluated by using 2 M NaCl as the eluant. PCE fibers could be easily separated from the adsorption solution without the energy-intensive centrifugation for the regeneration. The desorption efficiency could reach as high as 99.6%. After ten adsorption–desorption cycles, the removal efficiency of PCE fibers toward ReO_4^- was still $\geq 95.0\%$ (Figure S16, Supporting Information).

Excess competing anions including NO_3^- , SO_4^{2-} , and so on co-exist with $^{99}\text{TcO}_4^-$ in the waste streams and disturb the selective capture of $^{99}\text{TcO}_4^-$. The adsorption selectivity results are displayed in Figure 3d. When the treated solution contained competing anions with the same molar concentration as ReO_4^- , PCE fibers still adsorbed ReO_4^- with high removal efficiencies exceeding 99%. We also measured the adsorption of ReO_4^- with excess NO_3^- and SO_4^{2-} (Figure 3e,f). When the NO_3^- : ReO_4^- and SO_4^{2-} : ReO_4^- molar ratios were 100:1, the removal efficiencies toward ReO_4^- were still as high as 85.7% and 89.6%, respectively, comparable to some of advanced porous adsorbents such as ImPOP-1,^[32] SCU-CPN-1,^[7] and SCU-103.^[42] PCE fibers had a hydrophobic nature with a water contact angle of 94.5° (Figure S17, Supporting Information) due to their rough surface architecture and grafted hydrophobic ethyl chains. The hydrophobic environment makes that PCE fibers favor the less hydrophilic and larger anions such as $^{99}\text{TcO}_4^-/\text{ReO}_4^-$ rather than NO_3^- and SO_4^{2-} , following the anti-Hofmeister bias.^[5,7,15] The results confirm that PCE fibers have strong affinity and high selectivity toward ReO_4^- . The removal of ReO_4^- under different pH values were tested to show the fibers' adsorption ability in acidic and alkaline conditions (Figure S18, Supporting Information). At selected pH range (2–11), the removal efficiencies were high up to 90%. In certain types of nuclear waste streams, the pH values are either highly acidic or alkaline. Thus, we investigated the adsorption performance of PCE fibers toward ReO_4^- in 3 M HNO_3 solution and 1 M NaOH solution to estimate their potential application in real extreme conditions. As shown in the FTIR spectra of alkali-treated and acid-treated PCE fibers (Figure S19, Supporting Information), their compositions were still almost identical to that of the original sample. More importantly, at the solid–liquid ratio of 50:1, 56.5%, and 77.9% of ReO_4^- were removed from the 3 M HNO_3 and 1 M NaOH solution (Figure S20, Supporting Information), respectively, suggesting their promising $^{99}\text{TcO}_4^-$ uptake ability from highly acidic or alkaline nuclear waste. For nuclear waste stream treatment, the radiation exposure is inevitable. Both dry and wet PCE fibers were exposed to 50 and 200 kGy of ^{60}Co gamma irradiation to evaluate their radiation stability. Impressively, the FT–IR spectra of PCE fibers after these radiation processing were almost unchanged in comparison with the pristine sample (Figure S21, Supporting Information). Additionally, the irradiation had little effect on the ReO_4^- adsorption (Figure S22, Supporting Information). Encouraged by the excellent adsorption performance of PCE fibers, we further assessed their potential application in a simplified simulated Hanford Low Activity Waste (LAW) Melter Recycle Stream that contains high concentrations of complicated interfering anions (Table S7, Supporting Information). It was found that 84.5% of ReO_4^- ions was removed from the simulated waste

stream when the solid to liquid ratio was 10 g L^{-1} , which is better than the removal using ZBC (79.1% at a solid/liquid ratio of 10),^[43] NDTB-1 (13.0% at a solid/liquid ratio of 5),^[13] and SCU-101 (75.2% at a solid/liquid ratio of 10).^[17]

2.3. $^{99}\text{TcO}_4^-/\text{ReO}_4^-$ Removal Mechanism Analysis

The adsorption mechanism of PCE fibers toward ReO_4^- was investigated using the testing apparatus characterization. In the FT–IR spectrum of PCE fibers after ReO_4^- adsorption (PCE-Re), a new peak at 914 cm^{-1} corresponding to the Re–O stretching vibration appeared (Figure 4a).^[18,44] In the elemental mapping images and EDX spectrum, Cl was almost replaced by Re (Figure S15, Supporting Information). After the ReO_4^- adsorbed PCE fibers were regenerated by 2 M NaCl, the FT–IR spectrum of PCE fibers resumed the original curve and the Re–O stretching vibration disappeared. These results indicate that the ion exchange from Cl^- to ReO_4^- is the main driving force for the adsorption process. The XPS was also conducted to analyze the adsorption mechanism. In the XPS survey spectrum of PCE fibers after ReO_4^- adsorption, Re 4f and Re 4d peaks appeared and Cl 2p peak almost disappeared owing to the ion exchange process (Figure S23, Supporting Information). The Re 4f core-level spectra showed two fitting peaks at 47.3 and 45.0 eV corresponding to Re 4f_{2/5} and Re 4f_{7/7} (Figure 4b), respectively, which confirms the oxidation state of Re(VII).^[31,45] Additionally, compared with that of KReO_4 salts, the binding energy of Re 4f_{7/7} had a red shift from 45.4 to 45.0 eV because of the increase in electron density from the interaction between ReO_4^- ions and quaternary ammonium groups.^[6,32] EXAFS data were collected to further illustrate the local structure around Re atoms. Raw and Fourier transforms of Re L3 edge k³-weighted spectra of ReO_4^- adsorbed PCE fibers are displayed in Figure 4c,d. According to the fitting results, there was a Re–O shell with a distance (*R*) of 1.74 Å and the coordination number (*N*) of Re–O was evaluated to be 3.76, which are close to those of the referenced NaReO_4 (*R* = 1.74 Å, *N* = 4; Table S8, Supporting Information).^[7] The EXAFS results agree with the XPS data, indicating that Re species keep the +7 oxidation states and no Re(VII) reduction is involved in the adsorption process.

To quantitatively understand the intrinsic adsorption force and selectivity for $^{99}\text{TcO}_4^-/\text{ReO}_4^-$ adsorption by PCE fibers, density functional theory (DFT) calculations were performed. The interaction between the positively charged fragment ($[\text{N}(\text{C}_2\text{H}_5)_4]^+$, abbreviated as F^+) in PCE fibers and anions such as $\text{TcO}_4^-/\text{ReO}_4^-$, NO_3^- , SO_4^{2-} , and Cl^- were analyzed. Their stable adsorption structures are displayed in Figure 4e. The detailed calculation processes are provided in Supporting Information. The binding energies (E_b) in $\text{F}^+\cdots\text{TcO}_4^-$ ($-8.14 \text{ kcal mol}^{-1}$) and $\text{F}^+\cdots\text{ReO}_4^-$ ($-9.01 \text{ kcal mol}^{-1}$) were much higher than that in $\text{F}^+\cdots\text{Cl}^-$ ($-3.27 \text{ kcal mol}^{-1}$). The large energy differences dominated the ion exchange from Cl^- to TcO_4^- or ReO_4^- , which is the intrinsic driving force for the $^{99}\text{TcO}_4^-/\text{ReO}_4^-$ adsorption by PCE fibers. On the other hand, it could be seen that the calculated binding energies of $\text{F}^+\cdots\text{TcO}_4^-$ and $\text{F}^+\cdots\text{ReO}_4^-$ were also higher than those of $\text{F}^+\cdots\text{NO}_3^-$ ($-4.92 \text{ kcal mol}^{-1}$) and $\text{F}^+\cdots\text{SO}_4^{2-}$ ($-6.53 \text{ kcal mol}^{-1}$) mainly due to the less hydrophilic nature of $\text{TcO}_4^-/\text{ReO}_4^-$

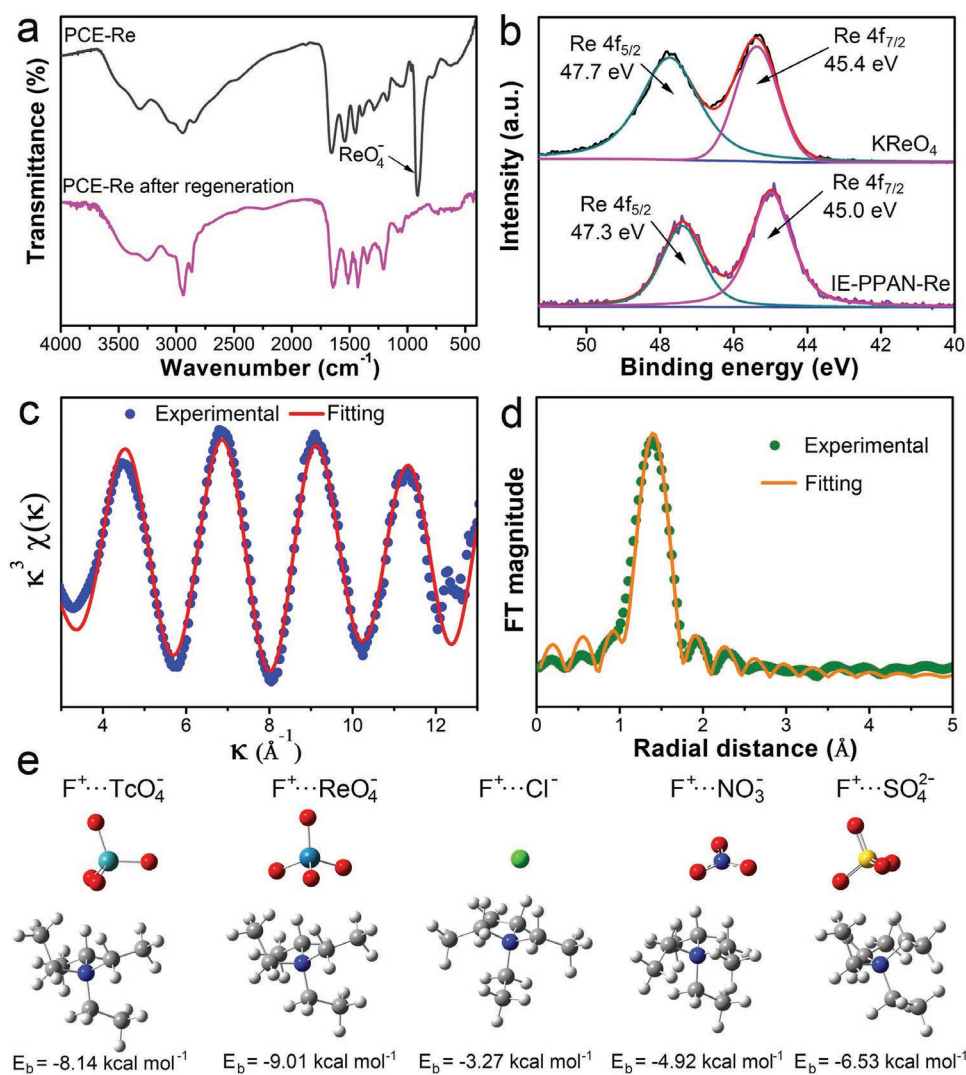


Figure 4. a) FT-IR spectra of ReO₄⁻ adsorbed PCE fibers (PCE-Re) before and after the regeneration. b) XPS analysis of the Re 4f from KReO₄ and PCE-Re. c) Raw and d) Fourier transforms of Re L₃ edge k₃-weighted EXAFS spectra of PCE-Re. e) Optimized adsorption complexes and binding energies of F⁺⋯TcO₄⁻, F⁺⋯ReO₄⁻, F⁺⋯Cl⁻, F⁺⋯NO₃⁻, and F⁺⋯SO₄²⁻. The gray, white, blue, red, yellow, green, cyan, and dark cyan balls represent C, H, N, O, S, Cl, Tc, and Re atoms, respectively.

compared to NO₃⁻ and SO₄²⁻. This indicates that PCE fibers trend to adsorb TcO₄⁻/ReO₄⁻ in the coexistence of NO₃⁻ and SO₄²⁻ leading to the good selectivity.

2.4. Dynamic Adsorption Experiments

For the engineering requirement, adsorbents are usually packed into columns for the dynamic ⁹⁹TcO₄⁻/ReO₄⁻ removal. However, the reported advanced porous materials with powder form are difficult in manipulating the column mode due to the clogging, aggregation, and possible secondary contamination.^[46,47] Thus, adsorbents with engineered form are more suitable as column adsorption or membrane filtration in practical application. Compared with granular ion exchange resins, electrospun fibers are used in not only column adsorption but also membrane filtration. In this study, PCE fiber membrane was employed as

adsorption membrane for dynamic ReO₄⁻ removal via the filtration (Figure 5a). After the PCE fibers treated 120 mL of ReO₄⁻ solution, the residual concentration of Re in the filtrate was only 15.1 ppb, suggesting their excellent filtration ability. If c_f/c₀ = 0.05 is defined as the breakthrough point, the breakthrough volume was 240 mL in the first filtration cycle. The used PCE fiber membrane in the filtration experiments is 35 mg. It means that PCE fibers can treat the ReO₄⁻ solution (removal efficiency > 95%) with mass of ≈6860 times over the adsorbent mass. After the saturated adsorption, the membrane was eluted by 2 M NaCl to desorb ReO₄⁻ through the filtration. Through calculating the adsorption amount and the desorption amount, 97.14% of ReO₄⁻ ions were eluted down after the regeneration. After five filtration-desorption cycles, the breakthrough volume by PCE fiber membrane was still 223 mL indicating its good recycling capacity (Figure 5b). Furthermore, the simulated Hanford LAW stream was also forced to pass through the PCE fiber membrane. Due

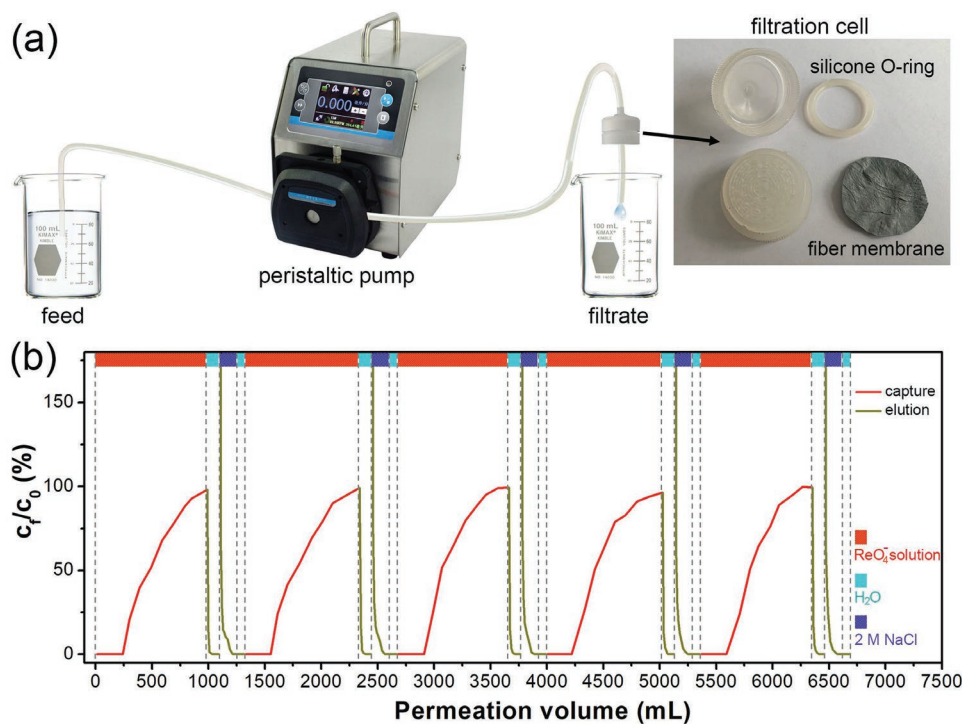


Figure 5. a) Experimental facility for dynamic ReO_4^- removal via the membrane adsorption. b) Dynamic adsorption and elution analysis of ReO_4^- by PCE fibers ($C_0 = 25.0 \text{ mg g}^{-1}$, $m_{\text{adsorbent}} = 35.0 \text{ mg}$, flow rate = 5.0 mL min^{-1}).

to the complex co-existing ions and high ReO_4^- concentration, the breakthrough volume was 21 mL (Figure S24, Supporting Information), which means that PCE fibers treat the simulated wastes (ReO_4^- removal efficiency > 95%) with mass of 600 times over the adsorbent mass. The PCE fibers after the dynamic ReO_4^- removal from simulated Hanford LAW stream was regenerated by 2 M NaCl. After the regeneration, the dynamic removal performance could be also maintained (Figure S24, Supporting Information). The dynamic adsorption results showed that PCE fibers held promise in practical radioactive waste treatment application.

3. Conclusion

In summary, we demonstrated herein the rational design of porous cationic electrospun PCE fibers with the engineered form for $^{99}\text{TcO}_4^-/\text{ReO}_4^-$ uptake. Due to the porous architectures and hyperbranched grafting structures, PCE fibers with the highly accessibility and the abundance of adsorption sites exhibited excellent adsorption properties toward $^{99}\text{TcO}_4^-/\text{ReO}_4^-$ including adsorption kinetics, adsorption capacity, adsorption selectivity, reusability, and stability under acidic, alkaline, and radiative conditions. Dynamic filtration experiments confirmed that PCE fiber membrane effectively trapped ReO_4^- with good recyclability. These results suggest that PCE fibers have great potential to be applied for ^{99}Tc removal in many areas.

Supporting Information

Supporting Information is available from the Wiley Online Library or from the author.

Acknowledgements

This work was financially supported by the National Natural Science Foundation of China (52003040, 22075040, 22131004 and U21A20330), Science and Technology Research Project of Education Department of Jilin Province (JJKH20211281KJ), Natural Science Foundation of Department of Science and Technology of Jilin Province (YDZJ202101ZYTS060), the “111” project (B18012) and the Fundamental Research Funds for the Central Universities (2412020FZ010).

Conflict of Interest

The authors declare no conflict of interest.

Data Availability Statement

The data that support the findings of this study are available from the corresponding author upon reasonable request.

Keywords

dynamic removal, fibrous adsorbents, hyperbranched quaternary ammonium groups, pertechnetate, porous

Received: January 17, 2022

Revised: February 27, 2022

Published online:

- [1] C. W. Abney, R. T. Mayes, T. Saito, S. Dai, *Chem. Rev.* **2017**, *117*, 13935.
[2] H. Yang, X. Liu, M. Hao, Y. Xie, X. Wang, H. Tian, G. I. N. Waterhouse, P. E. Kruger, S. G. Telfer, S. Ma, *Adv. Mater.* **2021**, *33*, 2106621.

- [3] Q. Sun, L. Zhu, B. Aguila, P. K. Thallapally, C. Xu, J. Chen, S. Wang, D. Rogers, S. Ma, *Nat. Commun.* **2019**, *10*, 1646.
- [4] Y. Wang, D. Han, S. Zhong, X. Li, H. Su, T. Chu, J. Peng, L. Zhao, J. Li, M. Zhai, *J. Hazard. Mater.* **2021**, *401*, 123354.
- [5] J. Li, B. Li, N. Shen, L. Chen, Q. Guo, L. Chen, L. He, X. Dai, Z. Chai, S. Wang, *ACS Cent. Sci.* **2021**, *7*, 1441.
- [6] Y. Wang, M. Xie, J. Lan, L. Yuan, J. Yu, J. Li, J. Peng, Z. Chai, J. K. Gibson, M. Zhai, W. Shi, *Chem* **2020**, *6*, 2796.
- [7] J. Li, X. Dai, L. Zhu, C. Xu, D. Zhang, M. A. Silver, P. Li, L. Chen, Y. Li, D. Zuo, H. Zhang, C. Xiao, J. Chen, J. Diwu, O. K. Farha, T. E. Albrecht-Schmitt, Z. Chai, S. Wang, *Nat. Commun.* **2018**, *9*, 3007.
- [8] L. Mei, F. Li, J. Lan, C. Wang, C. Xu, H. Deng, Q. Wu, K. Hu, L. Wang, Z. Chai, J. Chen, J. K. Gibson, W. Shi, *Nat. Commun.* **2019**, *10*, 1532.
- [9] R. Alberto, G. Bergamaschi, H. Braband, T. Fox, V. Amendola, *Angew. Chem., Int. Ed.* **2012**, *51*, 9772.
- [10] D. Banerjee, D. Kim, M. J. Schweiger, A. A. Krugerc, P. K. Thallapally, *Chem. Soc. Rev.* **2016**, *45*, 2724.
- [11] K. Kang, N. Shen, Y. Wang, L. Li, M. Zhang, X. Zhang, L. Lei, X. Miao, S. Wang, C. Xiao, *Chem. Eng. J.* **2022**, *427*, 130942.
- [12] C. Xiao, A. Khayambashi, S. Wang, *Chem. Mater.* **2019**, *31*, 3863.
- [13] S. Wang, P. Yu, B. A. Purse, M. J. Orta, J. Diwu, W. H. Casey, B. L. Phillips, E. V. Alekseev, W. Depmeier, D. T. Hobbs, T. E. Albrecht-Schmitt, *Adv. Funct. Mater.* **2012**, *22*, 2241.
- [14] D. Sheng, L. Zhu, C. Xu, C. Xiao, Y. Wang, Y. Wang, L. Chen, J. Diwu, J. Chen, Z. Chai, T. E. Albrecht-Schmitt, S. Wang, *Environ. Sci. Technol.* **2017**, *51*, 3471.
- [15] H. J. Da, C. X. Yang, X. P. Yan, *Environ. Sci. Technol.* **2019**, *53*, 5212.
- [16] L. He, S. Liu, L. Chen, X. Dai, J. Li, M. Zhang, F. Ma, C. Zhang, Z. Yang, R. Zhou, Z. Chai, S. Wang, *Chem. Sci.* **2019**, *10*, 4293.
- [17] L. Zhu, D. Sheng, C. Xu, X. Dai, M. A. Silver, J. Li, P. Li, Y. Wang, Y. Wang, L. Chen, C. Xiao, J. Chen, R. Zhou, C. Zhang, O. K. Farha, Z. Chai, T. E. Albrecht-Schmitt, S. Wang, *J. Am. Chem. Soc.* **2017**, *139*, 14873.
- [18] J. Li, L. Chen, N. Shen, R. Xie, M. V. Sheridan, X. Chen, D. Sheng, D. Zhang, Z. Chai, S. Wang, *Sci. China Chem.* **2021**, *64*, 1251.
- [19] J. Xue, T. Wu, Y. Dai, Y. Xia, *Chem. Rev.* **2019**, *119*, 5298.
- [20] Z. Zhu, W. Wang, D. Qi, Y. Luo, Y. Liu, Y. Xu, F. Cui, C. Wang, X. Chen, *Adv. Mater.* **2018**, *30*, 1801870.
- [21] C. J. Luo, S. D. Stoyanov, E. Stride, E. Pelan, M. Edirisinghe, *Chem. Soc. Rev.* **2012**, *41*, 4708.
- [22] R. Zhao, Y. Tian, S. Li, T. Ma, H. Lei, G. Zhu, *J. Mater. Chem. A* **2019**, *7*, 22559.
- [23] J. Yan, K. Dong, Y. Zhang, X. Wang, A. A. Aboalhasan, J. Yu, B. Ding, *Nat. Commun.* **2019**, *10*, 5584.
- [24] Y. Wang, W. Li, S. Chao, Y. Li, X. Li, D. He, C. Wang, *Chem. Res. Chinese Universities* **2020**, *36*, 1292.
- [25] R. Zhao, X. Li, B. Sun, Y. Li, Y. Li, R. Yang, C. Wang, *J. Mater. Chem. A* **2017**, *5*, 1133.
- [26] Z. Zhu, P. Wu, G. Liu, X. He, B. Qi, G. Zeng, W. Wang, Y. Sun, F. Cui, *Chem. Eng. J.* **2017**, *313*, 957.
- [27] Z. Zhang, N. Chu, Y. Shen, C. Li, R. Liu, *Colloid Polym. Sci.* **2021**, *299*, 25.
- [28] W. Li, Y. Y. Liu, Y. Bai, J. Wang, H. Pang, *J. Hazard. Mater.* **2020**, *395*, 122692.
- [29] Y. Yuan, S. Zhao, J. Wen, D. Wang, X. Guo, L. Xu, X. Wang, N. Wang, *Adv. Funct. Mater.* **2019**, *29*, 1805380.
- [30] M. Huang, L. Kan, W. Zhao, Y. Wang, Y. Xiong, W. Shan, Z. Lou, *Chem. Eng. J.* **2021**, *421*, 127763.
- [31] Q. H. Hu, W. Jiang, R. P. Liang, S. Lin, J. D. Qiu, *Chem. Eng. J.* **2021**, *419*, 129546.
- [32] Z. W. Liu, B. H. Han, *Environ. Sci. Technol.* **2020**, *54*, 216.
- [33] M. L. Wang, T. T. Jiang, Y. Lu, H. J. Liu, Y. Chen, *J. Mater. Chem. A* **2013**, *1*, 5923.
- [34] K. Xie, Z. Dong, M. Zhai, W. Shi, L. Zhao, *Appl. Surf. Sci.* **2021**, *551*, 149406.
- [35] H. Geng, C. Zhang, M. Tao, N. Ma, W. Zhang, *J. CO₂ Util.* **2021**, *49*, 101559.
- [36] W. Cao, Z. Wang, Q. Zeng, C. Shen, *Appl. Surf. Sci.* **2016**, *389*, 404.
- [37] Y. Zhang, G. Chen, L. Wu, K. Liu, H. Zhong, Z. Long, M. Tong, Z. Yang, S. Dai, *Chem. Commun.* **2020**, *56*, 3309.
- [38] B. Li, Y. Zhang, D. Ma, Z. Xing, T. Ma, Z. Shi, X. Ji, S. Ma, *Chem. Sci.* **2016**, *7*, 2138.
- [39] T. G. Levitskaia, E. L. Campbell, G. B. Hall, S. Chatterjee, D. Boglaienko, D. D. Reilly, M. A. Carlson, *J. Environ. Chem. Eng.* **2020**, *8*, 104155.
- [40] L. Fu, J. Zu, H. Wang, X. Pan, *J. Radioanal. Nucl. Chem.* **2019**, *322*, 2043.
- [41] M. Ding, L. Chen, Y. Xu, B. Chen, J. Ding, R. Wu, C. Huang, Y. He, Y. Jin, C. Xia, *Chem. Eng. J.* **2020**, *380*, 122581.
- [42] N. Shen, Z. Yang, S. Liu, X. Dai, C. Xiao, K. Taylor-Pashow, D. Li, C. Yang, J. Li, Y. Zhang, M. Zhang, R. Zhou, Z. Chai, S. Wang, *Nat. Commun.* **2020**, *11*, 5571.
- [43] H. Hu, L. Sun, Y. Gao, T. Wang, Y. Huang, C. Lv, Y. F. Zhang, Q. Huang, X. Chen, H. Wu, *J. Hazard. Mater.* **2020**, *387*, 121670.
- [44] X. Li, L. Chai, J. Ren, L. Jin, H. Wang, Y. Li, S. Ma, *Polym. Chem.* **2022**, *13*, 156.
- [45] X. Li, Y. Li, H. Wang, Z. Niu, Y. He, L. Jin, M. Wu, H. Wang, L. Chai, A. M. Al-Enizi, A. Nafady, S. F. Shaikh, S. Ma, *Small* **2021**, *17*, 2007994.
- [46] Y. Chen, S. Zhang, S. Cao, S. Li, F. Chen, S. Yuan, C. Xu, J. Zhou, X. Feng, X. Ma, B. Wang, *Adv. Mater.* **2017**, *29*, 1606221.
- [47] B. Valizadeh, T. N. Nguyen, B. Smit, K. C. Stylianou, *Adv. Funct. Mater.* **2018**, *28*, 1801596.